ACCOUNTS
of chemical research

RNA Folding Pathways and the Self-Assembly of Ribosomes

SARAH A. WOODSON*

T. C. Jenkins Department of Biophysics, Johns Hopkins University, 3400 North Charles Street, Baltimore, Maryland 21218, United States

RECEIVED ON FEBRUARY 23, 2011

CONSPECTUS

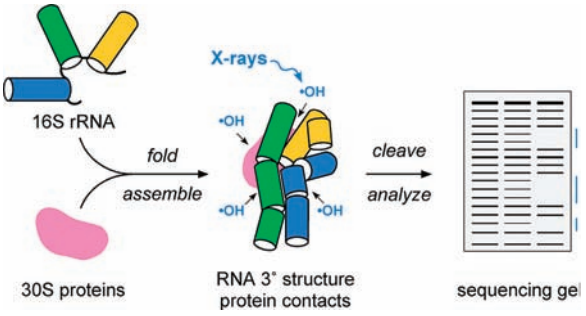

Many RNAs do not directly code proteins but are nonetheless indispensable to cellular function. These strands fold into intricate three-dimensional shapes that are essential structures in protein synthesis, splicing, and many other processes of gene regulation and expression. A variety of biophysical and biochemical methods are now showing, in real time, how ribosomal subunits and other ribonucleoprotein complexes assemble from their molecular components. Footprinting methods are particularly useful for studying the folding of long RNAs: they provide quantitative information about the conformational state of each residue and require little material. Data from footprinting complement the global information available from small-angle X-ray scattering or cryo-electron microscopy, as well as the dynamic information derived from single-molecule Förster resonance energy transfer (FRET) and NMR methods. In this Account, I discuss how we have used hydroxyl radical footprinting and other experimental methods to study pathways of RNA folding and 30S ribosome assembly.

Hydroxyl radical footprinting probes the solvent accessibility of the RNA backbone at each residue in as little as 10 ms, providing detailed views of RNA folding pathways in real time. In conjunction with other methods such as solution scattering and single-molecule FRET, time-resolved footprinting of ribozymes showed that stable domains of RNA tertiary structure fold in less than 1 s. However, the free energy landscapes for RNA folding are rugged, and individual molecules kinetically partition into folding pathways that lead through metastable intermediates, stalling the folding or assembly process.

Time-resolved footprinting was used to follow the formation of tertiary structure and protein interactions in the 16S ribosomal RNA (rRNA) during the assembly of 30S ribosomes. As previously observed in much simpler ribozymes, assembly occurs in stages, with individual molecules taking different routes to the final complex. Interactions occur concurrently in all domains of the 16S rRNA, and multistage protection of binding sites of individual proteins suggests that initial encounter complexes between the rRNA and ribosomal proteins are remodeled during assembly.

Equilibrium footprinting experiments showed that one primary binding protein was sufficient to stabilize the tertiary structure of the entire 16S 5′-domain. The rich detail available from the footprinting data showed that the secondary assembly protein S16 suppresses non-native structures in the 16S 5′-domain. In doing so, S16 enables a conformational switch distant from its own binding site, which may play a role in establishing interactions with other domains of the 30S subunit. Together, the footprinting results show how protein-induced changes in RNA structure are communicated over long distances, ensuring cooperative assembly of even very large RNA–protein complexes such as the ribosome.

Introduction

Long noncoding RNAs fold into diverse and complex tertiary structures that allow them to act as enzymes or metabolic sensors, often in complex with one or more proteins. Central among these are the rRNAs that form the cellular machinery for protein translation. Growing cells

Published on the Web 06/29/2011 www.pubs.acs.org/accounts
10.1021/ar2000474

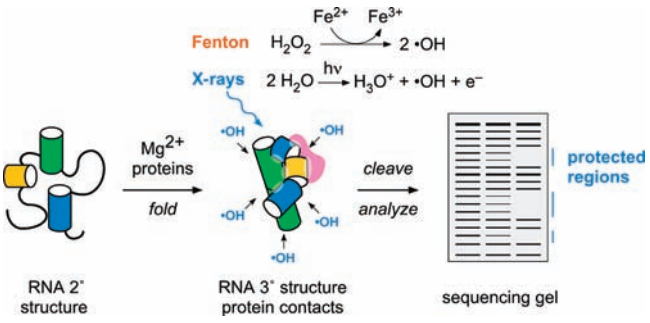

FIGURE 1. Hydroxyl radical footprinting of RNA and protein interactions. Ribose sugars buried by RNA tertiary interactions or protein contacts are protected from attack by hydroxyl radical, producing a gap or "footprint" in the distribution of cleaved products.[9] Radicals are produced by the Fenton reaction or X-ray photolysis of water; strand scission products are analyzed and quantified by primer extension with reverse transcriptase. Base oxidation products are not readily detected by this method.

require large numbers of new ribosomes to satisfy the demand for protein synthesis.[1] Consequently, all cells regulate the biosynthesis of ribosome components in response to growth and stress, while a host of additional assembly and maturation factors ensure the quality of the finished product.[2,3] A confluence of biophysical and biochemical methods are now revealing the details of how ribosomal subunits and other ribonucleoprotein complexes (RNP) assemble in real time from their molecular components.[4,5]

In this Account, I discuss how my laboratory has used hydroxyl radical footprinting and other experimental methods to study pathways of RNA folding and 30S ribosome assembly. The detailed information on RNA folding intermediates provided by footprinting experiments has provided evidence for induced fit in RNA−protein recognition and revealed how RNA-binding proteins can communicate RNA structural changes over long distances. In the future, such information will help to reveal how assembly is coordinated with pre-rRNA maturation, intracellular trafficking, and quality control pathways.

Visualizing RNA Folding Pathways with Hydroxyl Radical Footprinting

Classic studies of 30S ribosome reconstitution by Nomura and colleagues revealed that proteins join the complex in a hierarchy.[6] Subsequently, chemical modification experiments, along with cross-linking and other methods, showed that ribosomal proteins change the conformation of the rRNA in specific ways, and that protein-induced refolding of the rRNA is the basis for the cooperativity of subunit assembly.[7]

Footprinting methods are particularly useful for studying the folding of long RNAs, because they provide quantitative information about the conformational state of each residue and require little material.[8] Hydroxyl radical cleavage of the RNA backbone is proportional to the solvent accessibility of the C4′ and C5′ positions in the ribose (Figure 1)[9] and can be used to map the inside of a folded RNA or the extent of protein binding with single nucleotide precision.[10,11] The details provided by footprinting complement global information obtained from small-angle X-ray scattering (SAXS) or cryo-electron microscopy and dynamic information obtained from single-molecule Förster resonance energy transfer (FRET) and NMR methods.

To follow RNA folding in real time, it is necessary to carry out the hydroxyl radical cleavage reaction quickly, in order to obtain "snap shots" of the RNA tertiary interactions as they form. Mark Chance and Michael Brenowitz's laboratories developed a synchrotron X-ray beamline for time-resolved footprinting of RNA, which produces hydroxyl radical footprints within 1−10 ms irradiation of the sample.[12] Brenowitz and co-workers subsequently developed a rapid-quench protocol that uses the Fenton reaction (Fe(II)−EDTA) to produce hydroxyl radical.[13]

Since footprinting methods probe the average conformation of the molecules in the solution at a given time, a clear footprint is only visible when >10% of molecules form exactly the same molecular contacts. Consequently, this method does not detect compact intermediates that are dynamic in structure or regions of the structure that are heterogeneously folded within the population. As discussed below, such compact intermediates can be detected by SAXS or by FRET, providing a more complete picture of the folding process.

RNA Folding Principles from Ribozymes

To understand RNP assembly mechanisms, it is helpful to first consider how RNAs fold in the absence of proteins. Real-time hydroxyl radical footprinting of the *Tetrahymena* group I ribozyme showed that large domains of RNA tertiary structure can form in a few seconds or less (Figure 2).[14] However, the catalytic center of the ribozyme folds slowly (>1 min) in vitro,[15,16] due to mispairing of a pseudoknot, which traps about 90% of the RNA in misfolded intermediates.[17] Because these misfolded intermediates are also stabilized by peripheral tertiary interactions, refolding times are long.[18−20]

Importantly, a few molecules avoid misfolding and fold correctly with a rate of ~1 s^{-1} at 37 °C, which was observed directly by single-molecule FRET.[21−23] Thus, studies on the *Tetrahymena* ribozyme revealed a second important

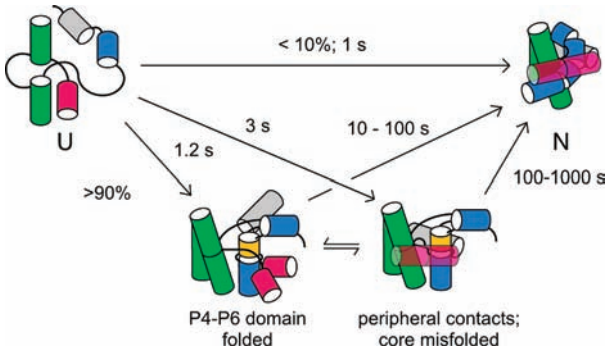

FIGURE 2. Folding pathway of the *Tetrahymena* ribozyme. Time-resolved footprinting[14,25] showed that tertiary interactions in the P4–P6 domain (green) form in ~1 s, more rapidly than contacts in peripheral helices (pink and gray) and in the P3–P9 domain (blue), due to mispairing of the P3 helix (gold).[17] The ensemble of unfolded structures (U) partitions among parallel pathways, with 5–10% of molecules folding directly to the native state (N).[21]

principle, which is that RNA populations fold in parallel along different paths, some leading directly to the native structure and others detouring through metastable intermediates (Figure 2).[24] Footprinting results reflect the superposition of these folding pathways, making heterogeneously folded regions appear unstructured. If the pathways are not too varied, however, the dominant folding intermediates can be inferred by deconvolution of changes in backbone accessibility over time.[25]

Third, the "outside-in" folding pattern of the *Tetrahymena* ribozyme revealed by the time-resolved footprinting studies suggested that the late folding intermediates are compact. Time-resolved SAXS experiments on the *Tetrahymena* ribozyme[26] and other RNAs[27,28] showed that initial collapse transitions, which bring the helical domains together, occur in 1–15 ms. However, in several ribozymes and riboswitches studied so far, collapse is followed by further conformational adjustments that allow the double helices to pack tightly and specifically with one another.[29]

Fourth, compact structures are formed by reorientation of the double helices around flexible junctions in the secondary structure. In some RNAs, bending of helix junctions can limit the rate of helix docking.[30,31] Because helix junctions are important for defining RNA architecture, it is not surprising that many primary assembly proteins in the 30S ribosome bind helix junctions in the 16S rRNA. Single-molecule experiments showed that binding of protein S15 to a three-helix junction correlates with correct helix orientation.[32]

Finally, tertiary interactions between helices begin to form during the collapse transition, and these bias the folding intermediates toward the native structure.[33,34] This is likely critically important for the assembly of large RNA complexes, because the tertiary structure provides the additional information needed to constrain the structures of early folding intermediates. RNA-binding proteins can also interact with compact folding intermediates, suggesting that such loosely folded states contribute directly to RNP assembly.[33]

Multistage Assembly of 30S Ribosome by Time-Resolved Hydroxyl Radical Footprinting

Because the hierarchical addition of proteins to ribosomal subunits described by the Nomura assembly map[35] arises from structural changes in the rRNA due to protein binding,[7] we expected RNA folding principles to play a large role in assembly. Few proteins contact each other directly in the mature bacterial 30S subunit.[36] However, each protein not only stabilizes the rRNA within its immediate binding site, it also stimulates structural changes in adjacent residues that help recruit other proteins to the complex.

The basis for cooperative assembly was illustrated by biophysical studies from Williamson and co-workers, showing that protein S15 captures and stabilizes the junction between helices 20, 21, and 22 in the central domain, holding them in the correct orientation.[32,37] S15 binding also stabilizes interactions with helix 23 that form the binding site of the S6–S18 dimer,[38] which in turn organizes the binding site for S11. The thermodynamic cooperativity for binding of central domain proteins is associated with a reduction in the unfavorable entropy change associated with protein binding, consistent with increased preorganization of the rRNA.[39]

We used time-resolved hydroxyl radical footprinting to visualize changes in the rRNA structure during 30S assembly in real time.[40] *Escherichia coli* 16S rRNA was first refolded in 20 mM $MgCl_2$, then 30S subunit proteins were added using a rapid quench instrument. Complexes were exposed at various intervals to a synchrotron X-ray beam for 10 ms (Figure 3). This approach captured emerging RNA tertiary interactions and RNA–protein interactions from 20 ms to 180 s of assembly.

As in the *Tetrahymena* ribozyme, some 16S residues became more than 65% protected within the first 50 ms of the assembly reaction, while other residues required several minutes to fold.[40] Not only were residues in different domains of the rRNA protected at different times, but individual residues were protected with more than one rate constant. For many residues, a burst of protection in the first 50 ms was

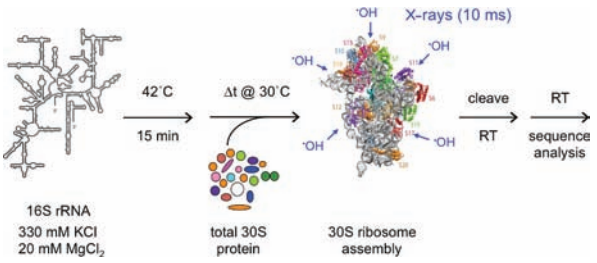

FIGURE 3. X-ray footprinting of 30S ribosome assembly. The evolution of RNA and RNA–protein interactions was probed from 20 ms to 120 s, using a 10 ms X-ray pulse.[40] Native *E. coli* 16S rRNA was prefolded in reconstitution buffer before addition of native *E. coli* 30S proteins (TP30). Quantitation of primer extension products revealed multistage folding of individual residues throughout the 16S rRNA.

followed by much slower saturation of the backbone interactions. These results suggested not only that assembly involves different intermediate complexes but also that different rRNA molecules assemble along different paths, as inferred earlier from the binding kinetics of 30S proteins.[41]

Residues in every domain of the 16S rRNA were protected rapidly, showing that the domains of the 16S rRNA assemble concurrently in vitro.[40] Some of the fast folding regions corresponded to helix junctions that are partly stable in the absence of proteins, while others mapped to protein binding sites, including primary assembly proteins S4, S8, S15, and S7. Regions of the 16S rRNA that were protected most slowly included irregularly folded regions of the rRNA, residues that form long-range interactions between structural domains, and residues that form the central pseudoknot and the mRNA decoding site in the mature 30S subunit. These last results agreed with reconstitution experiments showing that the pseudoknot forms in the late stages of 30S assembly.[42]

Direction of Assembly

In nature, ribosomal subunits are assembled during transcription, and assembly is intimately coupled with processing and maturation of the pre-rRNA.[3] However, our footprinting experiments on the native 16S rRNA showed that each region of the rRNA folds and binds proteins at the same time.[40] This suggests that the 16S domains can assemble in any order, as long as the rRNA can adopt the correct conformation. Indeed, recent genetic experiments showed that circularly permuted 16S and 23S genes maintain viability, demonstrating that the usual 5′ to 3′ order or pre-rRNA transcription is not obligatory.[43]

On the other hand, there is evidence that the usual 5′ to 3′ direction of assembly is preferred in vitro, particularly at 30 °C.[44] Moreover, 5′ and central domain proteins accelerate association of proteins with the 3′ domain in pulse–chase experiments, suggesting that prior assembly of these domains is advantageous.[45] The observed gradient of assembly may reflect the propensity of each 16S domain to fold correctly. The 5′ domain of the *E. coli* 16S rRNA is rich in RNA interactions and can fold independently of proteins in a few seconds.[46] Not surprisingly, quantitative mass spectrometry and pulse–chase experiments showed that 5′ domain proteins are incorporated into 30S subunits fastest.[41] By contrast, the central and 3′ domains cannot fold properly without their protein ligands, and proteins that bind these domains are incorporated more slowly in pulse–chase experiments.[41,45]

Because the RNA and protein interactions observed by footprinting represent unproductive as well as productive assembly intermediates, rapid protection of certain residues in the 3′ domain could represent false starts. Indeed, the 3′ domain folded 100 times more slowly when the 16S rRNA was renatured at 30 °C instead of 42 °C in time-resolved footprinting experiments and is more susceptible to base modification interference,[47] suggesting that assembly can proceed more rapidly if metastable conformations in the rRNA are overcome.

More recently, Williamson and co-workers used a high-throughput strategy for capturing electron microscopy images to visualize stable assembly intermediates of the 30S ribosome.[48] Many early complexes resembled the body or 5′ domain, while later complexes contained a mixture of platform and head structures that correspond to the 16S central and 3′ domains, respectively. These results are consistent with a general 5′ to 3′ direction of assembly. However, the heterogeneity of the assembly intermediates again indicates assembly can follow different paths.[48] An interesting question is the extent to which this heterogeneity occurs in the cell and whether redundant assembly pathways and suboptimality are retained over the course of evolution.

Induced Fit in RNA–Protein Recognition

One of the most striking observations from time-resolved footprinting of 30S ribosome assembly was that the interfaces between the rRNA and individual ribosomal proteins form at different rates. For example, residues in helices 16 and 17 that contact the C-terminal domain of protein S4 were protected in 0.1–1 s, while residues in helices 16 and 18 that interact with the N-terminal region of S4 were protected more slowly (Figure 4).[40] This suggested that initial encounter complexes between the ribosomal proteins and the RNA contain only a subset of the native contacts and must

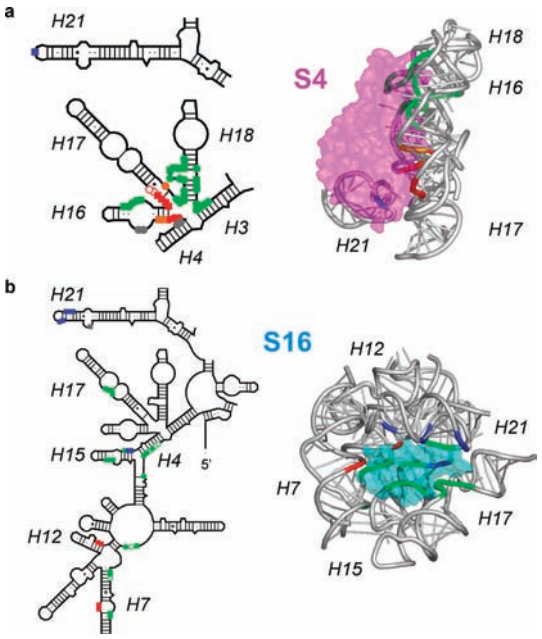

FIGURE 4. Induced fit in rRNA–protein interactions. Different residues in a single 30S protein binding site are protected with different rate constants, when probed by X-ray footprinting. (a) Residues contacted by protein S4 in mature 30S subunits colored according to the rate of protection: red, $\geq 20\ s^{-1}$; orange, $2-20\ s^{-1}$; green, $0.2-2\ s^{-1}$; blue, $0.01-0.2\ s^{-1}$. (b) Residues contacted by protein S16, colored as in panel a. Reproduced from ref 40 with permission. Copyright 2008 Nature Publishing Group.

undergo further structural changes. In general, the slowest rates of protection from hydroxyl radical cleavage were most similar to protein binding rates measured by pulse–chase mass spectrometry,[41] suggesting that it is these slower steps that commit proteins to further steps of 30S assembly.

Interestingly, the N-terminal region of S4 is disordered in the free protein,[49] raising the possibility that changes in protein structure occur after the initial binding event. Although RNA binding proteins may promote folding simply by selecting conformations already present in the ensemble of unliganded structures, nonspecific protein binding may induce new conformations or increase the dynamics of the RNA, lowering the energy barriers to refolding.[50−52] Most RNA binding proteins contain large numbers of basic amino acid residues, and electrostatic attraction to the RNA may drive the initial formation of nonspecific and dynamic encounter complexes, as suggested for the RNA recognition motif (RRM) protein U1A.[53,54]

Global Stabilization of rRNA Structure by Ribosomal Proteins

To understand in detail how proteins stabilize the tertiary structure of the rRNA, we used equilibrium hydroxyl radical footprinting to measure the effect of 5′ domain proteins on the folding intermediates. The 16S 5′ domain forms the body of the 30S subunit and binds three primary assembly proteins (S4, S17, and S20), as well as one secondary assembly protein, S16.[55−57] S4, S17, and S20 each organize a different helix junction in the 5′ domain (Figure 5), while S16 binds at the interface between the "upper" and "lower" halves of the 5′ domain. Protein S12 also forms part of 30S body but binds 16S 5′ domain fragments weakly.

The Mg^{2+} concentration required to refold RNA generally correlates with the stability of its tertiary structure. Therefore, by reconstituting 5′ domain RNP complexes in a range of Mg^{2+} concentration, we could determine how much the proteins stabilize specific RNA tertiary contacts.[58] Although the 16S 5′ domain RNA can fold in the absence of proteins in high $MgCl_2$,[46] the ribosomal proteins stabilized the RNA structure as expected, allowing tertiary interactions in the 5′ domain RNA to form in 5 mM $MgCl_2$.[58]

Surprisingly, S4 or S17 alone stabilized tertiary interactions throughout the 5′ domain, allowing many of the expected RNA tertiary contacts to form in low Mg^{2+}.[59] Indirect stabilization of an RNA tertiary domain by a single protein has been observed for ribozymes, such as group I introns and RNase P, that form strong networks of RNA tertiary interactions able to propagate the effects of protein binding to distant regions of the complex.[60−62] However, it was not expected that ribosomal proteins would have such global effects. By contrast, RNAs with weaker tertiary interactions, such as signal recognition particle (SRP)[63,64] or telomerase,[65] appear to recruit their protein ligands in a stricter hierarchy.

Remote Activation of a Conformational Switch by S16

The detail in the footprinting data revealed how the ribosomal proteins change the structure of the rRNA, altering the free energy landscape for assembly. An important observation was that each primary assembly protein preferentially stabilizes a different subset of RNA conformations, producing different footprints in intermediate Mg^{2+} concentrations.[59] A second important observation was that certain residues were protected in discrete stages when all three primary assembly proteins S4, S17, and S20 were present.[58] Some residues were incrementally protected in two transitions, while others were partially protected in no Mg^{2+}, exposed at intermediate Mg^{2+} (~1 mM), and fully protected in high Mg^{2+} (5–20 mM) (Figure 5). These oscillations occurred in helix 18 and at the tip of helix 12, which

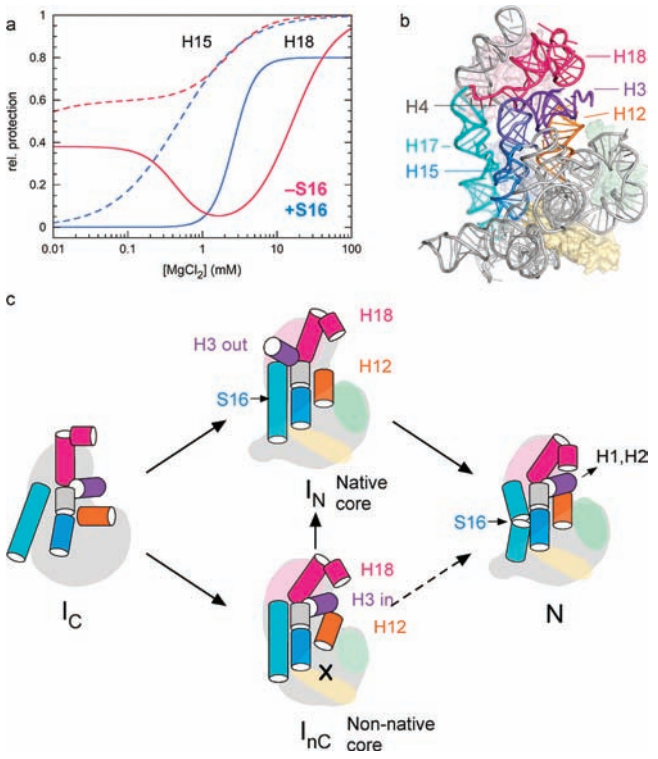

FIGURE 5. S16-dependent conformational switch. (a) Proteins that bind the 16S 5′ domain (body) stabilize RNA tertiary interactions, lowering the Mg^{2+} concentration required for protection from hydroxyl radical cleavage.[58,59] Fitted curves for protection of residues in helix 15 (nt 378; dashed lines) and helix 18 (nt 501–502; solid lines) in the presence of S4, S17, and S20, without S16 (pink) or with S16 (blue). (b) Exposure of helix 18 can be explained by movement of helix 3 (purple) during assembly. Ribbon (pdb 2avy)[75] shows 16S nt 24–562 with proteins as pastel surfaces; S4 (pink), S17 (green), S20 (yellow), S16 (blue). (c) Minimal model for 5′ domain assembly, involving intermediate RNPs with native (I_N) or non-native (I_{nC}) configuration in the lower half of the domain near helices 6, 6a, 10, and 15. Helix 3 is displaced in I_N, then moves back into position in the native complex (N). S16 smooths the path of assembly by favoring I_N over I_{nC} and by stabilizing N. Reproduced from ref 58 with permission. Copyright 2009 Nature Publishing Group.

contact opposite faces of helix 3 in the upper half of the 5′ domain, and were best explained by dislocation of helix 3 at an intermediate stage of assembly and repositioning of helix 3 at the final stage of assembly (Figure 5).[58]

From these results, we draw several conclusions about the mechanism of assembly. First, assembly intermediates with different structures accumulate simultaneously, in agreement with energy landscape models for the assembly process. Second, interactions surrounding helix 3 are remodeled during the assembly process.[58] This is important because helix 3 joins the 5′ domain to the central domain and docking of helix 3 stabilizes the conformation of the 530-loop pseudoknot in helix 18, a critical element of the mRNA decoding center in the mature 30S ribosome.[66]

Third, the secondary assembly protein S16 smooths out this conformational change, by depopulating intermediates in which helix 3 is docked prematurely at low Mg^{2+} (I_{nC}, Figure 5). Moreover, as the Mg^{2+} concentration is raised, S16 stabilizes the native RNP, in which helix 3 is docked and the pseudoknot in helix 18 is properly folded. Remarkably, the S16 binding site straddles a tertiary interaction motif between helices 15 and 17, ~30 Å away from helix 3. These results demonstrate how the effects of protein binding can be communicated over long distances in the ribosome, allowing secondary assembly proteins such as S16 to influence RNA interactions remotely.

Chaperones, Assembly Factors, and Quality Control

Ribosome assembly is far more efficient in the cell than in the test tube, with synthesis, assembly, and maturation requiring about 2 min on average in rapidly growing *E. coli*.[67] Efforts to understand how cellular factors overcome the barriers to rRNA folding and assembly are now underway.[3,68] Although it is well established that ribosomal proteins stabilize the folded rRNA, many ribosomal proteins such as S12 and S1, along with other RNA binding proteins such as StpA and Hfq, also accelerate RNA refolding.[69] Thus, ribosomal proteins could aid assembly by lowering the kinetic barriers to RNA conformational changes, in addition to selecting native-like intermediates. The dnaK protein chaperone has also been implicated in 30S ribosome assembly.[70,71]

While nonspecific RNA and protein chaperones likely function at early stages of assembly, specific assembly factors, including modification and processing enzymes act at later stages of the process.[3,68] Most 30S assembly factors are not essential except under stress conditions, consistent with the notion that assembly can take different paths, bypassing steps that are inefficient or blocked. An interesting exception is the essential GTPase Era, which binds the 3′ end of the 16S rRNA[72] and facilitates entry of many 3′ domain proteins.[45] Depletion of another GTPase RsgA (YjeQ) also results in the accumulation of immature subunits lacking several ribosomal proteins, in which the "neck" and mRNA decoding center are perturbed.[73] RsgA is reported to facilitate dissociation of RbfA,[74] an assembly factor that binds the same region. These results suggest that assembly of the 16S 3′ domain (head) and neck, which correspond to the slowest and most heterogeneous steps of assembly in vitro, require either direct facilitation or active surveillance in the cell.

Conclusions

Experimental methods and theoretical models for studying RNA folding pathways are being adapted to reveal how large cellular complexes are assembled from their molecular components. Given the many noncoding RNAs that function as cellular enzymes or that participate in regulatory pathways, methods for interrogating RNA conformation will remain in demand. Hydroxyl radical footprinting probes the solvent accessibility of individual residues in RNA in a few milliseconds, allowing RNP assembly reactions to be followed in real time. The detailed information from footprinting studies complements results from fluorescence spectroscopy, microscopy, solution scattering, and mass spectrometry.

Consistent with studies on smaller ribozymes, time-resolved footprinting of the 16S rRNA showed that 30S subunit assembly is multiphase, suggesting that individual complexes take different routes to the final structure. Each domain of the 16S rRNA assembles concurrently, with many stable RNA and RNA−protein interactions forming within the first 50−100 ms. Individual proteins protect their binding sites with more than one rate constant, suggesting that induced fit of RNA−protein contacts contributes to the hierarchy of 30S assembly. Finally, the connectivity in the rRNA structure allows bound proteins to influence the structure of the rRNA over long distances, driving specific conformational changes that help create the mRNA decoding site of the 30S subunit. In the future, in vivo footprinting methods promise further insight into how the folding and assembly of RNA−protein complexes coordinate with each phase of RNP biogenesis.

The author thanks the many people in her laboratory who contributed to this work over the years and collaborations past and present with M. Brenowitz, R. Briber, M. Chance, and D. Thirumalai, without whom this work would not have been possible. This work was funded by the NIGMS.

BIOGRAPHICAL INFORMATION

Sarah Woodson received her Ph.D. at Yale University in 1987 with Donald Crothers, then did postdoctoral work with Thomas Cech at the University of Colorado before joining the faculty of the University of Maryland in 1990. In 1999, she moved to Johns Hopkins University where she is a professor in the Department of Biophysics.

FOOTNOTES

*E-mail swoodson@jhu.edu; tel 410-516-2015; fax 410-516-4118.

REFERENCES

1 Warner, J. R.; Vilardell, J.; Sohn, J. H. Economics of ribosome biosynthesis. *Cold Spring Harbor Symp. Quant. Biol.* **2001**, *66*, 567–574.
2 Wilson, D. N.; Nierhaus, K. H. The weird and wonderful world of bacterial ribosome regulation. *Crit. Rev. Biochem. Mol. Biol.* **2007**, *42*, 187–219.
3 Kaczanowska, M.; Ryden-Aulin, M. Ribosome biogenesis and the translation process in Escherichia coli. *Microbiol. Mol. Biol. Rev.* **2007**, *71*, 477–494.
4 Woodson, S. A. RNA folding and ribosome assembly. *Curr. Opin. Chem. Biol.* **2008**, *12*, 667–673.
5 Williamson, J. R. Biophysical studies of bacterial ribosome assembly. *Curr. Opin. Struct. Biol.* **2008**, *18*, 299–304.
6 Held, W. A.; Ballou, B.; Mizushima, S.; Nomura, M. Assembly mapping of 30 S ribosomal proteins from Escherichia coli. Further studies. *J. Biol. Chem.* **1974**, *249*, 3103–3111.
7 Stern, S.; Powers, T.; Changchien, L. M.; Noller, H. F. RNA-protein interactions in 30S ribosomal subunits: Folding and function of 16S rRNA. *Science* **1989**, *244*, 783–790.
8 Weeks, K. M. Advances in RNA structure analysis by chemical probing. *Curr. Opin. Struct. Biol.* **2010**, *20*, 295–304.
9 Tullius, T. D.; Greenbaum, J. A. Mapping nucleic acid structure by hydroxyl radical cleavage. *Curr. Opin. Chem. Biol.* **2005**, *9*, 127–134.
10 Latham, J. A.; Cech, T. R. Defining the inside and outside of a catalytic RNA molecule. *Science* **1989**, *245*, 276–282.
11 Hsieh, M.; Brenowitz, M. Quantitative kinetics footprinting of protein-DNA association reactions. *Methods Enzymol.* **1996**, *274*, 478–492.
12 Ralston, C. Y.; Sclavi, B.; Sullivan, M.; Deras, M. L.; Woodson, S. A.; Chance, M. R.; Brenowitz, M. Time-resolved synchrotron X-ray footprinting and its application to RNA folding. *Methods Enzymol.* **2000**, *317*, 353–368.
13 Shcherbakova, I.; Mitra, S.; Beer, R. H.; Brenowitz, M. Following molecular transitions with single residue spatial and millisecond time resolution. *Methods Cell Biol.* **2008**, *84*, 589–615.
14 Sclavi, B.; Sullivan, M.; Chance, M. R.; Brenowitz, M.; Woodson, S. A. RNA folding at millisecond intervals by synchrotron hydroxyl radical footprinting. *Science* **1998**, *279*, 1940–1943.
15 Zarrinkar, P. P.; Williamson, J. R. Kinetic intermediates in RNA folding. *Science* **1994**, *265*, 918–924.
16 Zarrinkar, P. P.; Williamson, J. R. The kinetic folding pathway of the Tetrahymena ribozyme reveals possible similarities between RNA and protein folding. *Nat. Struct. Biol.* **1996**, *3*, 432–438.
17 Pan, J.; Woodson, S. A. Folding intermediates of a self-splicing RNA: Mispairing of the catalytic core. *J. Mol. Biol.* **1998**, *280*, 597–609.
18 Pan, J.; Woodson, S. A. The effect of long-range loop-loop interactions on folding of the Tetrahymena self-splicing RNA. *J. Mol. Biol.* **1999**, *294*, 955–965.
19 Russell, R.; Zhuang, X.; Babcock, H. P.; Millett, I. S.; Doniach, S.; Chu, S.; Herschlag, D. Exploring the folding landscape of a structured RNA. *Proc. Natl. Acad. Sci. U.S.A.* **2002**, *99*, 155–160.
20 Treiber, D. K.; Rook, M. S.; Zarrinkar, P. P.; Williamson, J. R. Kinetic intermediates trapped by native interactions in RNA folding. *Science* **1998**, *279*, 1943–1946.
21 Pan, J.; Thirumalai, D.; Woodson, S. A. Folding of RNA involves parallel pathways. *J. Mol. Biol.* **1997**, *273*, 7–13.
22 Zhuang, X.; Bartley, L. E.; Babcock, H. P.; Russell, R.; Ha, T.; Herschlag, D.; Chu, S. A single-molecule study of RNA catalysis and folding. *Science* **2000**, *288*, 2048–2051.
23 Pan, J.; Deras, M. L.; Woodson, S. A. Fast folding of a ribozyme by stabilizing core interactions: Evidence for multiple folding pathways in RNA. *J. Mol. Biol.* **2000**, *296*, 133–144.
24 Thirumalai, D.; Woodson, S. A. Kinetics of folding of protein and RNA. *Acc. Chem. Res.* **1996**, *29*, 433–439.
25 Laederach, A.; Shcherbakova, I.; Liang, M. P.; Brenowitz, M.; Altman, R. B. Local kinetic measures of macromolecular structure reveal partitioning among multiple parallel pathways from the earliest steps in the folding of a large RNA molecule. *J. Mol. Biol.* **2006**, *358*, 1179–1190.
26 Russell, R.; Millett, I. S.; Tate, M. W.; Kwok, L. W.; Nakatani, B.; Gruner, S. M.; Mochrie, S. G.; Pande, V.; Doniach, S.; Herschlag, D.; Pollack, L. Rapid compaction during RNA folding. *Proc. Natl. Acad. Sci. U.S.A.* **2002**, *99*, 4266–4271.
27 Fang, X. W.; Pan, T.; Sosnick, T. R. Mg2+-dependent folding of a large ribozyme without kinetic traps. *Nat. Struct. Biol.* **1999**, *6*, 1091–1095.
28 Roh, J. H.; Guo, L.; Kilburn, J. D.; Briber, R. M.; Irving, T.; Woodson, S. A. Multistage collapse of a bacterial ribozyme observed by time-resolved small-angle X-ray scattering. *J. Am. Chem. Soc.* **2010**, *132*, 10148–10154.
29 Woodson, S. A. Compact intermediates in RNA folding. *Annu. Rev. Biophys.* **2010**, *39*, 61–77.
30 Schlatterer, J. C.; Kwok, L. W.; Lamb, J. S.; Park, H. Y.; Andresen, K.; Brenowitz, M.; Pollack, L. Hinge stiffness is a barrier to RNA folding. *J. Mol. Biol.* **2008**, *379*, 859–870.

31 Zhuang, X.; Kim, H.; Pereira, M. J.; Babcock, H. P.; Walter, N. G.; Chu, S. Correlating structural dynamics and function in single ribozyme molecules. *Science* **2002**, *296*, 1473–1476.

32 Ha, T.; Zhuang, X.; Kim, H. D.; Orr, J. W.; Williamson, J. R.; Chu, S. Ligand-induced conformational changes observed in single RNA molecules. *Proc. Natl. Acad. Sci. U.S.A.* **1999**, *96*, 9077–9082.

33 Webb, A. E.; Weeks, K. M. A collapsed state functions to self-chaperone RNA folding into a native ribonucleoprotein complex. *Nat. Struct. Biol.* **2001**, *8*, 135–140.

34 Chauhan, S.; Woodson, S. A. Tertiary interactions determine the accuracy of RNA folding. *J. Am. Chem. Soc.* **2008**, *130*, 1296–1303.

35 Nomura, M.; Held, W. A.: Reconstitution of ribosomes: Studies of ribosome structure, function, and assembly. In *Ribosomes*; Nomura, M., Tissieres, A., Lengyel, P., Eds.; Cold Spring Harbor Laboratory Press: Cold Spring Harbor, NY, 1974; pp 193−223.

36 Wimberly, B. T.; Brodersen, D. E.; Clemons, W. M., Jr.; Morgan-Warren, R. J.; Carter, A. P.; Vonrhein, C.; Hartsch, T.; Ramakrishnan, V. Structure of the 30S ribosomal subunit. *Nature* **2000**, *407*, 327–339.

37 Batey, R. T.; Williamson, J. R. Interaction of the Bacillus stearothermophilus ribosomal protein S15 with 16 S rRNA: I. Defining the minimal RNA site. *J. Mol. Biol.* **1996**, *261*, 536–549.

38 Agalarov, S. C.; Sridhar Prasad, G.; Funke, P. M.; Stout, C. D.; Williamson, J. R. Structure of the S15,S6,S18-rRNA complex: assembly of the 30S ribosome central domain. *Science* **2000**, *288*, 107–113.

39 Recht, M. I.; Williamson, J. R. RNA tertiary structure and cooperative assembly of a large ribonucleoprotein complex. *J. Mol. Biol.* **2004**, *344*, 395–407.

40 Adilakshmi, T.; Bellur, D. L.; Woodson, S. A. Concurrent nucleation of 16S folding and induced fit in 30S ribosome assembly. *Nature* **2008**, *455*, 1268–1272.

41 Talkington, M. W.; Siuzdak, G.; Williamson, J. R. An assembly landscape for the 30S ribosomal subunit. *Nature* **2005**, *438*, 628–632.

42 Holmes, K. L.; Culver, G. M. Mapping structural differences between 30S ribosomal subunit assembly intermediates. *Nat. Struct. Mol. Biol.* **2004**, *11*, 179–186.

43 Kitahara, K.; Suzuki, T. The ordered transcription of RNA domains is not essential for ribosome biogenesis in Escherichia coli. *Mol. Cell* **2009**, *34*, 760–766.

44 Powers, T.; Daubresse, G.; Noller, H. F. Dynamics of in vitro assembly of 16 S rRNA into 30 S ribosomal subunits. *J. Mol. Biol.* **1993**, *232*, 362–374.

45 Bunner, A. E.; Beck, A. H.; Williamson, J. R. Kinetic cooperativity in Escherichia coli 30S ribosomal subunit reconstitution reveals additional complexity in the assembly landscape. *Proc. Natl. Acad. Sci. U.S.A.* **2010**, *107*, 5417–5422.

46 Adilakshmi, T.; Ramaswamy, P.; Woodson, S. A. Protein-independent folding pathway of the 16S rRNA 5′ domain. *J. Mol. Biol.* **2005**, *351*, 508–519.

47 Xu, Z.; Culver, G. M. Differential assembly of 16S rRNA domains during 30S subunit formation. *RNA* **2010**, *16*, 1990–2001.

48 Mulder, A. M.; Yoshioka, C.; Beck, A. H.; Bunner, A. E.; Milligan, R. A.; Potter, C. S.; Carragher, B.; Williamson, J. R. Visualizing ribosome biogenesis: parallel assembly pathways for the 30S subunit. *Science* **2010**, *330*, 673–677.

49 Sayers, E. W.; Gerstner, R. B.; Draper, D. E.; Torchia, D. A. Structural preordering in the N-terminal region of ribosomal protein S4 revealed by heteronuclear NMR spectroscopy. *Biochemistry* **2000**, *39*, 13602–13613.

50 Webb, A. E.; Rose, M. A.; Westhof, E.; Weeks, K. M. Protein-dependent transition states for ribonucleoprotein assembly. *J. Mol. Biol.* **2001**, *309*, 1087–1100.

51 Bokinsky, G.; Nivon, L. G.; Liu, S.; Chai, G.; Hong, M.; Weeks, K. M.; Zhuang, X. Two distinct binding modes of a protein cofactor with its target RNA. *J. Mol. Biol.* **2006**, *361*, 771–784.

52 Lewin, A. S.; Thomas, J., Jr.; Tirupati, H. K. Cotranscriptional splicing of a group I intron is facilitated by the Cbp2 protein. *Mol. Cell. Biol.* **1995**, *15*, 6971–6978.

53 Qin, F.; Chen, Y.; Wu, M.; Li, Y.; Zhang, J.; Chen, H. F. Induced fit or conformational selection for RNA/U1A folding. *RNA* **2010**, *16*, 1053–1061.

54 Katsamba, P. S.; Myszka, D. G.; Laird-Offringa, I. A. Two functionally distinct steps mediate high affinity binding of U1A protein to U1 hairpin II RNA. *J. Biol. Chem.* **2001**, *276*, 21476–21481.

55 Stern, S.; Changchien, L. M.; Craven, G. R.; Noller, H. F. Interaction of proteins S16, S17, and S20 with 16 S ribosomal RNA. *J. Mol. Biol.* **1988**, *200*, 291–299.

56 Weitzmann, C. J.; Cunningham, P. R.; Nurse, K.; Ofengand, J. Chemical evidence for domain assembly of the Escherichia coli 30S ribosome. *FASEB J.* **1993**, *7*, 177–180.

57 Brodersen, D. E.; Clemons, W. M., Jr.; Carter, A. P.; Wimberly, B. T.; Ramakrishnan, V. Crystal structure of the 30 S ribosomal subunit from Thermus thermophilus: structure of the proteins and their interactions with 16 S RNA. *J. Mol. Biol.* **2002**, *316*, 725–768.

58 Ramaswamy, P.; Woodson, S. A. S16 throws a conformational switch during assembly of 30S 5′ domain. *Nat. Struct. Mol. Biol.* **2009**, *16*, 438–445.

59 Ramaswamy, P.; Woodson, S. A. Global stabilization of rRNA structure by ribosomal proteins S4, S17, and S20. *J. Mol. Biol.* **2009**, *392*, 666–677.

60 Caprara, M. G.; Mohr, G.; Lambowitz, A. M. A tyrosyl-tRNA synthetase protein induces tertiary folding of the group I intron catalytic core. *J. Mol. Biol.* **1996**, *257*, 512–531.

61 Weeks, K. M.; Cech, T. R. Protein facilitation of group I intron splicing by assembly of the catalytic core and the 5′ splice site domain. *Cell* **1995**, *82*, 221–230.

62 Biswas, R.; Ledman, D. W.; Fox, R. O.; Altman, S.; Gopalan, V. Mapping RNA-protein interactions in ribonuclease P from Escherichia coli using disulfide-linked EDTA-Fe. *J. Mol. Biol.* **2000**, *296*, 19–31.

63 Doudna, J. A.; Batey, R. T. Structural insights into the signal recognition particle. *Annu. Rev. Biochem.* **2004**, *73*, 539–557.

64 Menichelli, E.; Isel, C.; Oubridge, C.; Nagai, K. Protein-induced conformational changes of RNA during the assembly of human signal recognition particle. *J. Mol. Biol.* **2007**, *367*, 187–203.

65 Stone, M. D.; Mihalusova, M.; O'Connor C, M.; Prathapam, R.; Collins, K.; Zhuang, X. Stepwise protein-mediated RNA folding directs assembly of telomerase ribonucleoprotein. *Nature* **2007**, *446*, 458–461.

66 Powers, T.; Noller, H. F. A functional pseudoknot in 16S ribosomal RNA. *EMBO J.* **1991**, *10*, 2203–2214.

67 Lindahl, L. Intermediates and time kinetics of the in vivo assembly of Escherichia coli ribosomes. *J. Mol. Biol.* **1975**, *92*, 15–37.

68 Connolly, K.; Culver, G. Deconstructing ribosome construction. *Trends Biochem. Sci.* **2009**, *34*, 256–263.

69 Rajkowitsch, L.; Chen, D.; Stampfl, S.; Semrad, K.; Waldsich, C.; Mayer, O.; Jantsch, M. F.; Konrat, R.; Blasi, U.; Schroeder, R. RNA chaperones, RNA annealers, and RNA helicases. *RNA Biol.* **2007**, *4*, 118–130.

70 Maki, J. A.; Schnobrich, D. J.; Culver, G. M. The DnaK chaperone system facilitates 30S ribosomal subunit assembly. *Mol. Cell* **2002**, *10*, 129–138.

71 Al Refaii, A.; Alix, J. H. Ribosome biogenesis is temperature-dependent and delayed in Escherichia coli lacking the chaperones DnaK or DnaJ. *Mol. Microbiol.* **2009**, *71*, 748–762.

72 Tu, C.; Zhou, X.; Tropea, J. E.; Austin, B. P.; Waugh, D. S.; Court, D. L.; Ji, X. Structure of ERA in complex with the 3′ end of 16S rRNA: Implications for ribosome biogenesis. *Proc. Natl. Acad. Sci. U.S.A.* **2009**, *106*, 14843–14848.

73 Jomaa, A.; Stewart, G.; Martin-Benito, J.; Zielke, R.; Campbell, T. L.; Maddock, J. R.; Brown, E. D.; Ortega, J. Understanding ribosome assembly: The structure of in vivo assembled immature 30S subunits revealed by cryo-electron microscopy. *RNA* **2011**, *17*, 697–709.

74 Goto, S.; Kato, S.; Kimura, T.; Muto, A.; Himeno, H. RsgA releases RbfA from 30S ribosome during a late stage of ribosome biosynthesis. *EMBO J.* **2011**, *30*, 104–114.

75 Schuwirth, B. S.; Borovinskaya, M. A.; Hau, C. W.; Zhang, W.; Vila-Sanjurjo, A.; Holton, J. M.; Cate, J. H. Structures of the bacterial ribosome at 3.5 A resolution. *Science* **2005**, *310*, 827–834.